Magn Reson Mater Phy (2011) 24:43–50
DOI 10.1007/s10334-010-0234-7

RESEARCH ARTICLE

Adapted random sampling patterns for accelerated MRI

Florian Knoll · Christian Clason · Clemens Diwoky · Rudolf Stollberger

Received: 13 January 2010 / Revised: 29 October 2010 / Accepted: 19 November 2010 / Published online: 7 January 2011

Abstract
Objective Variable density random sampling patterns have recently become increasingly popular for accelerated imaging strategies, as they lead to incoherent aliasing artifacts. However, the design of these sampling patterns is still an open problem. Current strategies use model assumptions like polynomials of different order to generate a probability density function that is then used to generate the sampling pattern. This approach relies on the optimization of design parameters which is very time consuming and therefore impractical for daily clinical use.
Materials and methods This work presents a new approach that generates sampling patterns by making use of power spectra of existing reference data sets and hence requires neither parameter tuning nor an a priori mathematical model of the density of sampling points.
Results The approach is validated with downsampling experiments, as well as with accelerated in vivo measurements. The proposed approach is compared with established sampling patterns, and the generalization potential is tested by using a range of reference images. Quantitative evaluation is performed for the downsampling experiments using RMS differences to the original, fully sampled data set.
Conclusion Our results demonstrate that the image quality of the method presented in this paper is comparable to that of an established model-based strategy when optimization of the model parameter is carried out and yields superior results to non-optimized model parameters. However, no random sampling pattern showed superior performance when compared to conventional Cartesian subsampling for the considered reconstruction strategy.

Keywords Accelerated imaging · Parallel imaging · Variable density sampling · Random sampling

F. Knoll (✉) · C. Diwoky · R. Stollberger
Institute of Medical Engineering, Graz University of Technology, Kronesgasse 5, 8010 Graz, Austria
e-mail: florian.knoll@tugraz.at

C. Clason
Institute for Mathematics and Scientific Computing, University of Graz, Heinrichstrasse 36, 8010 Graz, Austria

Introduction

Parallel Imaging (PI) is a well-established strategy for scan time reduction in MRI, and methods like SENSE [1] and GRAPPA [2] are already routinely used in clinical examinations. While conventional Cartesian subsampling is still the gold standard in most applications, alternative sampling patterns have been investigated for many years. Examples include non-Cartesian imaging strategies like radials [3] or spirals [4] and variable density sampling patterns [5–8].

Within the framework of compressed sensing, Lustig et al. [9,10] proposed the idea of randomized Cartesian subsampling. These randomized sampling patterns can be generated from Monte-Carlo simulations. With this approach, a probability density function (pdf) is constructed, and sampling pattern indices are drawn randomly according to that density. This leaves the problem of designing a pdf that will generate a suitable sampling pattern, and especially of determining the correct ratio of low to high frequency sample points. A common approach uses a density function which is proportional to a power of the distance from the origin in k-space. However, such strategies require optimization of one or even more design parameters that have a great influence on the reconstruction quality and depend on a suitably chosen mathematical model involving these parameters.

The goal of this work is to show that it is possible to construct an adapted random sampling pattern from a pdf that

is generated by using measured k-space data as a reference, which automatically ensures an appropriate distribution of sample points. These sampling patterns are then used for conventional parallel imaging.

Theory

Random sampling patterns are one of the key ingredients in compressed sensing. They allow variable density sampling by distributing the sampling points according to a specified probability density function (pdf). Their main advantage is the fact that the resulting subsampling artifacts are incoherent.

In their work on compressed sensing, Lustig et al. [9] used a density function based on a polynomial function of the distance to the origin. Specifically, if k_y and k_z denote the k-space coefficients in the two phase encoding directions and N and M are the number of phase encoding steps in y and z direction, the pdf was given by $\left(1 - \frac{1}{\sqrt{2NM}}\sqrt{k_y^2 + k_z^2}\right)^p$ for a suitably chosen p. Since in general the magnitude of the Fourier coefficients of medical images does not obey a simple power law, this leaves open the question of choosing an appropriate exponent for the pdf which best approximates that distribution. Additionally, these sampling patterns usually contain an area with a user-defined radius around the center of k-space where all sampling points are included. It was shown for compressed sensing that this improves the reconstruction quality, as the fully sampled low frequency k-space information can be used to estimate phase variations [9]. It is even more important for autocalibrated parallel imaging methods, because the sample points at the center of k-space are used to obtain the necessary information about the coil sensitivities. Suboptimal choice of these design parameters can lead to significantly lower image quality.

We therefore propose to generate a pdf that is directly based on the power spectrum of a template image. It is our observation that a template taken from any reasonably similar medical image data set will give good results: For the purpose of generating a suitable sampling pattern, only an estimation of the ratio of low to high frequency sample points has to be obtained. This merely depends on a similar distribution of the magnitude of k-space values, not similarity of magnitude and phase, which would require agreement in anatomical details. This also corresponds to the findings in [5] for the generalization potential of one-dimensional variable density subsampling.

Specifically, the proposed method is as follows: Given a template image, we take the magnitude of its Fourier transform, scaled such that the integral is one. If multiple slices are acquired during this reference measurement, this step is repeated for all slices of the template data set, and the results are averaged to increase robustness. Of course, if 3D sampling is performed for the reference measurement, an inverse Fourier transform has to be applied in the slice direction prior to the estimation of the pdf. However, as demonstrated by the results of this work, the method has good generalization characteristics if only a single slice is used as a template. Using the template as a probability density function, we compute the corresponding cumulative probability density function (cdf). A random number uniformly distributed between 0 and 1 is then generated for each possible sampling point on a fixed uniform Cartesian grid defined by the desired image resolution. We accept a sampling point if the corresponding random number is less than the cdf for this coordinate. This is repeated until enough unique sampling points are generated such that the prescribed acceleration factor is reached. The whole procedure is repeated several times, and the sampling pattern with the least coherence is taken.

Materials and methods

Downsampling experiments

The goal of the first experiment was to evaluate the proposed method against established sampling patterns. A fully sampled T_2-weighted 2D turbo spin echo scan of the brain of a healthy volunteer was acquired on a clinical 3T scanner (Siemens Magnetom TIM Trio, Erlangen, Germany) with a 32 channel head coil. Written informed consent was obtained from all subjects prior to all examinations. Sequence parameters were repetition time TR = 5,000 ms, echo time TE = 99 ms, turbo factor 10, matrix size (x, y) = (256, 256), 10 slices with a slice thickness of 4 mm and an in-plane resolution of 0.86 × 0.86 mm. The raw data set was exported from the scanner and then subsampled, to simulate an accelerated acquisition. Downsampling was conducted with different sampling patterns. In all experiments, subsampling with reduction factors $R = 4$ and $R = 9$ was performed. For the proposed method, the pdf was created using a data set from a scan of a different volunteer with the same sequence parameters, which was acquired several weeks earlier. The results were compared to reconstructions using established sampling patterns: conventional Cartesian subsampling, 2D CAIPIRINHA [11] type patterns (which have shown to yield results superior to conventional sampling) and random sampling using the polynomial distribution [9] given above. Image reconstruction was performed using GRAPPA [2]. A 2D 5 × 5 GRAPPA kernel was used in all reconstructions, with Tikhonov regularization in the calibration step. To deal with random sampling patterns, the implementation described in [13] was used. All reconstructions were carried out slice by slice. Prior to image reconstruction, an SVD-based coil compression scheme was used to reduce the computational load. Twelve virtual channels were used in all experiments. To illustrate the artifacts introduced by the different sampling

patterns, conventional zero-filled images were also generated by using an inverse Fourier transform with density compensation corresponding to the nonuniform sampling pattern, followed by a sum of squares (SOS) combination of the individual coil images.

To test the generalization potential of the method, additional experiments were undertaken where different templates were used to generate the pdf. The same undersampled data set was used as in the comparison of different sampling patterns, and the following images were used as templates:

1. A single slice of the same data set, adjacent to the slice that was subsampled and reconstructed, was used. Therefore, the anatomy is very similar to that in the undersampled image.
2. A 90° clockwise rotation of template 1.
3. A single slice of the same data set as template 1, measured at a more cranial position. This leads to slight changes in the imaged anatomy as the ventricles are no longer in the field of view and slightly changes the size of the support of the image.
4. A single slice of a data set of a different volunteer, obtained with a different receive coil (12 channel head coil) with different image contrast. A gradient echo sequence was used with the following sequence parameters: repetition time TR = 68 ms, echo time TE = 5 ms, matrix size (x, y) = (256, 256), slice thickness of 5 mm and an in-plane resolution of 0.89 × 0.89 mm.
5. A single slice of the sample data set from template 4, measured at a more caudal position. This leads to fundamental changes of the imaged anatomy and represents situations when unexpected anatomy is present in the undersampled image.

The goal of the next experiment was to test the applicability of the proposed method for a different anatomy. A fully sampled 2D spin echo scan of the knee of a healthy volunteer was acquired at 3T, using an 8 channel knee coil. Sequence parameters were repetition time TR = 1,800 ms, echo time TE = 18 ms, matrix size (x, y) = (256, 256) covering a FOV of 150 × 150 mm, 10 slices with a slice thickness of 2 mm. The raw data set was exported from the scanner and compressed to 4 virtual channels by means of an SVD-based coil compression scheme after visual inspection of the singular values. A different slice from this data set was used as the template to generate the pdf. Downsampling was conducted with $R = 2$ and $R = 4$. This lower amount of acceleration in comparison with the previous experiments was used due to the lower number of receive channels of the knee coil.

Accelerated in vivo measurements

Accelerated measurements of the brain of a healthy volunteer were performed at 3T (Siemens Magnetom TIM Trio, Erlangen, Germany) with a 32 channel head coil. The 32 receive channels were again compressed to 12 virtual coils. A 3D gradient echo sequence was used that was modified by including a binary 2D mask that defined the randomized subsampled pattern. The following sequence parameters were used: repetition time TR = 30 ms, echo time TE = 6.4 ms, flip angle FA = 13°, matrix size (x, y, z) = (256, 256, 256), isotropic spatial resolution of 1 mm. Subsampling with reduction factors $R = 4$ and $R = 10$ was performed. In all cases, pre-calculated sampling patterns for transversal scans of the brain were used, which were generated with the use of a pdf that was obtained from a single slice-reference scan of a different volunteer several weeks before the accelerated measurements. The reference measurement was taken with a 2D gradient echo sequence and with different sequence parameters (repetition time TR = 20 ms, echo time TE = 3.5 ms, flip angle FA = 18°, matrix size (x, y) = (256, 256), slice thickness 3 mm) to test the robustness of the method. In addition, a 12-channel head coil was used instead of the 32-channel coil of the accelerated measurements. Raw data were exported from the scanner, a 1D Fourier transform was performed along the readout direction, and partitions orthogonal to this axis were reconstructed offline.

Results

Using the method presented in [9], random patterns with $(1 - r)^p$ polynomial distributions were generated for polynomial powers from 2 to 20 for acceleration factor $R = 4$ and 4–20 for $R = 9$, and the RMS difference of the corresponding GRAPPA reconstructions to the original unaccelerated image was calculated. All experiments were repeated 3 times, and the mean RMS values were calculated. The choice $p = 7$ resulted in the lowest RMS error for $R = 4$ while $p = 5$ was the optimal choice for $R = 9$.

Figure 1 displays undersampled k-spaces, zero-filled SOS images, GRAPPA reconstruction results and k-spaces of the reconstructions for all tested sampling patterns and subsampling factors. In the regular Cartesian case, 2D subsampling strategies of 2 × 2 and 3 × 3 with 10 additional center lines were used. Additionally, a $2 \times 2^{(1)}$ 2D CAIPIRINHA pattern (2 × 2 subsampling with a shift of $\Delta = 1$ from one sampling row k_y to the next) was used in the case of $R = 4$, and a $3 \times 3^{(2)}$ pattern for $R = 9$. To illustrate the importance of the optimization of the polynomial order p for the reconstruction quality, results are also shown for a non-optimized p. In general, reconstructions are free of artifacts for all sampling patterns with an acceleration factor of $R = 4$. At reduction factors of $R = 9$, visible residual folding artifacts remain for regular Cartesian sampling (indicated by arrows), which are slightly reduced for 2D CAIPIRINHA. All random patterns show incoherent aliasing. Image quality of optimized random

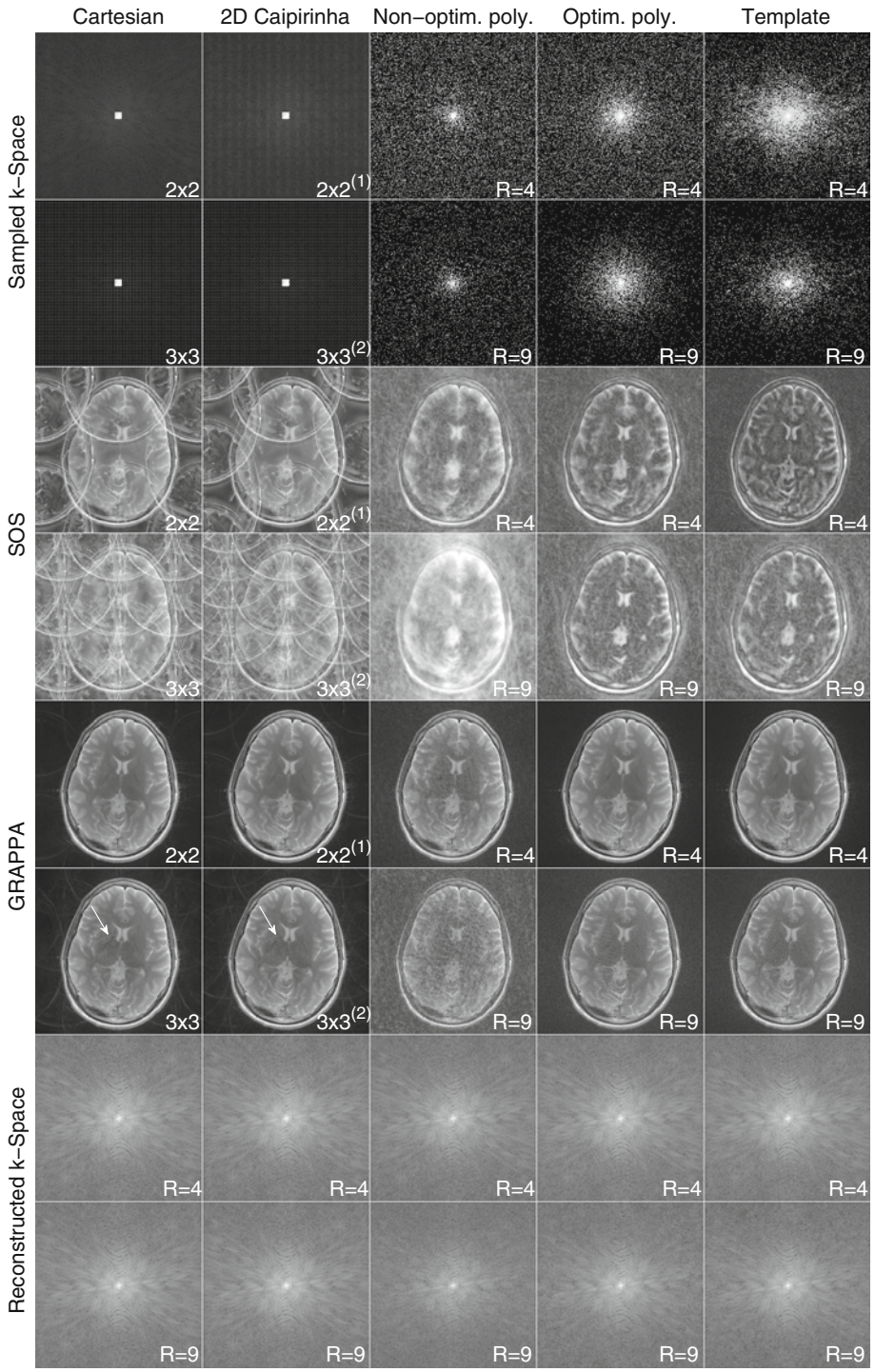

Fig. 1 Comparison of reconstruction results for different sampling patterns. Conventional Cartesian subsampling, 2D CAIPIRINHA type patterns, random sampling with optimized and non-optimized polynomial powers and the proposed template method. Residual aliasing artifacts for conventional Cartesian and 2D CAIPIRINHA patterns are indicated by *arrows*

patterns and the proposed template-based method are comparable. In contrast, the amount of aliasing in non-optimized polynomials is significantly higher.

Figure 2 shows the comparison when different templates are used to generate the sampling pattern. The template of the first column is very close to the undersampled target image, which means that it is not surprising that the generated sampling pattern represents a proper distribution of the ratio of high to low k-space points. However, even with increasing deviation from the exact anatomy of the first template, the generated patterns still allow to reconstruct images with almost the same quality. This behavior is the same for moderate ($R=4$) and high acceleration ($R=9$), which demonstrates that exact anatomical details do not have to be known when generating sampling patterns with the proposed method.

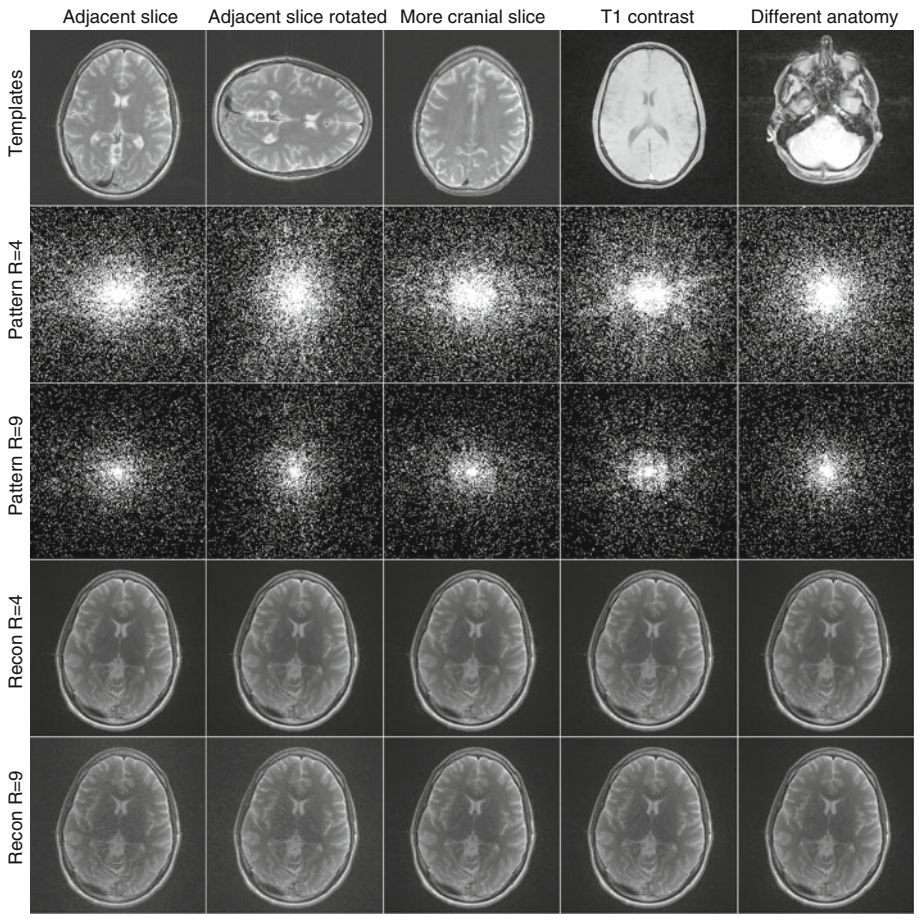

Fig. 2 Comparison of reconstruction results when different templates are used to generate the sampling pattern. An adjacent slice of the same data set as the undersampled slice (first column), a rotation of this slice (second column), a more cranial slice with slightly different anatomy and size of the head (third column), a data set of a different volunteer with different contrast (fourth column) and completely different anatomy (fifth column) were used. The templates, corresponding sampling patterns and GRAPPA reconstructions are shown for $R=4$ and $R=9$

Table 1 Quantitative evaluation of the GRAPPA reconstruction errors of the downsampling experiments with different sampling patterns

Pattern	$R=4$	$R=9$
Cartesian	0.046	0.091
2D CAIPIRINHA	0.045	0.086
Non-optimized polynomial	0.104 ± 0.016	0.300 ± 0.071
Optimized polynomial	0.042 ± 0.001	0.172 ± 0.037
Template	0.048 ± 0.004	0.165 ± 0.055

RMS differences (a.u.) to an SOS image from the original fully sampled data set are shown. The values for the random patterns are means with standard deviations over 10 different patterns for the same pdf

RMS differences to an SOS image of the original fully sampled data set are given in Table 1. For the random patterns, the experiments were each repeated 10 times for different sampling patterns generated from the same pdf, and mean values and standard deviations were calculated. With the exception of the unoptimized polynomial case, which has a much higher RMS error, all results are comparable for $R=4$. Optimized polynomials and the template-based method are comparable for $R=9$, and unoptimized polynomials again show the largest errors. Notably, the errors of both non-random patterns are significantly lower in this case.

Table 2 displays the results of RMS differences to the fully sampled reference data set when different templates were used. Like in the evaluation of Table 1, calculations were repeated 10 times for different sampling patterns generated from the same pdf. When compared with the results of Table 1, it can be seen that differences of the reconstruction error are far less pronounced for different templates than in the case of different sampling patterns. For both undersampling factors, the worst result was achieved in the case of the 90° rotation of the template. However, all errors are significantly lower than for the case of the non-optimized polynomial pattern in Table 1.

Figure 3 displays the template image, the fully sampled gold standard, sampling patterns, zero-filled SOS images, GRAPPA reconstructions and reconstructed k-spaces of the

Table 2 Quantitative evaluation of the GRAPPA reconstruction errors of the experiments with different templates

Pattern	$R=4$	$R=9$
T2w	0.048 ± 0.004	0.147 ± 0.048
T2w rotated	0.057 ± 0.011	0.173 ± 0.082
T2w different slice	0.047 ± 0.001	0.148 ± 0.039
T1w	0.051 ± 0.001	0.111 ± 0.017
Different anatomy	0.047 ± 0.001	0.107 ± 0.027

RMS differences (a.u.) to an SOS image from the original fully sampled data set are shown. Means with standard deviations over 10 different patterns for the same pdf are shown

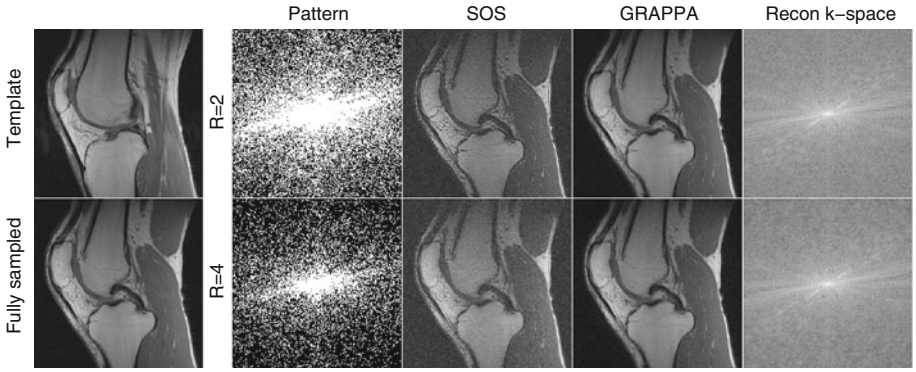

Fig. 3 The template image that was used to generate the sampling pattern, the fully sampled gold standard and reconstruction results of the experiments with the knee data set are shown. *Left* column: Used sampling pattern. *Middle left* column: undersampled and zero-filled (SOS) images. *Middle right* column: GRAPPA reconstruction. *Right* column: k-space of corresponding GRAPPA reconstruction. *Top* row: $R=2$. *Bottom* row: $R=4$

undersampled measurements of the knee for $R=2$ and $R=4$. RMS differences to the fully sampled gold standard are 0.049 ± 0.001 for $R=2$ and 0.077 ± 0.006 for $R=4$.

Figure 4 displays the template image, sampling patterns, zero-filled SOS images, GRAPPA reconstructions and reconstructed k-spaces of a single slice of the accelerated in-vivo experiments. The results show the same characteristics as the subsampling experiments. Reconstructions are free of artifacts for $R=4$, while results for $R=10$ already show some corruptions due to decrease in SNR and incoherent aliasing.

Discussion

The results from Fig. 1 as well as the RMS errors (Table 1) demonstrate that the proposed method leads to reconstructions with an image quality that is comparable to that of optimized polynomial patterns. It can also be seen that the quality of non-optimized polynomial distributions is clearly inferior, which illustrates the importance of the parameter optimization process for model-based strategies. However, finding an optimal parameter is a procedure with a very high

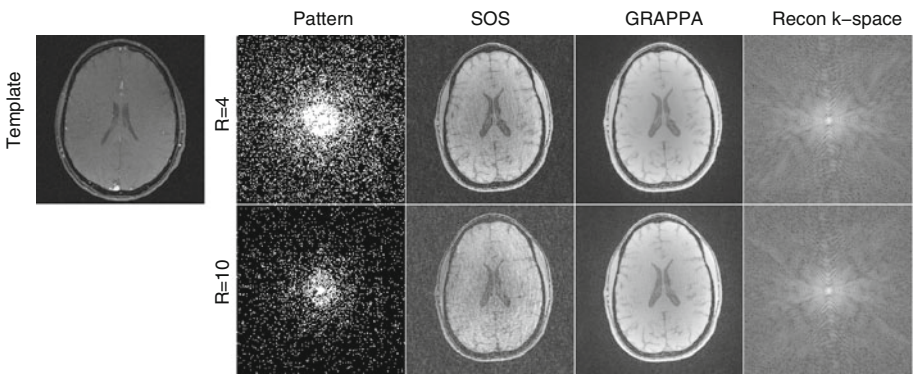

Fig. 4 The template image that was used to generate the sampling pattern and reconstruction results of accelerated in-vivo measurements for different subsampling factors are shown. *Left* column: Used sampling pattern. *Middle left* column: undersampled and zero-filled (SOS) images. *Middle right* column: GRAPPA reconstruction. *Right* column: k-space of corresponding GRAPPA reconstruction. *Top* row: $R=4$. *Bottom* row: $R=10$

computational load, because image reconstruction has to be repeated multiple times for the same data set. Additionally, in contrast to the proposed method where the patterns were generated with reference data, optimization of the design parameters was performed based on the data set to be subsampled and reconstructed. This approach was chosen in order to provide optimal conditions for the reference method, but it is of course unrealistic for a truly accelerated measurement in practice.

Another difficulty in parameter tuning is the need of a quantitative metric for image quality evaluation, since optimization based on visual inspection of the images will always lead to subjective results. In this work, the RMS difference to a fully sampled reference image was used. While this measure is widely used in MR image analysis, it does not capture image quality or diagnostic relevance of the reconstructed images very well and also requires a corresponding gold standard image usually not available in a clinical setting. Additionally, the success of finding suitable parameters depends on the correct choice of a mathematical model (such as $\left(1-\sqrt{k_x^2+k_y^2}\right)^p$ as opposed to $\left(k_x^2+k_y^2\right)^{-p}$, or even more complicated exponential models). In contrast, the proposed method does not require fixing a mathematical model a priori.

It is important to note that in the results from this work, the reconstructions from randomized sampling patterns in general were not superior to those of conventional Cartesian subsampling and 2D CAIPIRINHA. In the case of $R=9$, the RMS errors of random patterns were actually higher. The reason for this is that conventional parallel imaging strategies, like GRAPPA, do not explicitely exploit the properties of incoherent aliasing artifacts, in contrast to compressed sensing-based reconstruction methods. In order to make full use of random patterns, parallel imaging must be combined with a regularization method that enforces the removal of incoherent artifacts such as TV [12] or wavelets [13]. However, such a comparison of different reconstruction strategies is outside the scope of this paper. Another reason for residual artifacts in the case of the random patterns that were investigated in this work is the fact that the distances between sample points in the outer regions of k-space increase and "holes" appear in the sampling pattern, which are not completely covered by the extent of the GRAPPA reconstruction kernel. It is reasonable that image quality can be further increased by adding an additional constraint during the design of the sampling pattern, which ensures that a certain distance between adjacent sample points is not exceeded [13].

As demonstrated in the results from Fig. 2 and Table 2, the proposed method is very robust with respect to the choice of the reference data set, as only a similar distribution of the magnitude of k-space values is required, not similarity in image space. This distribution does not differ considerably for measurements of the same anatomical region, which is in agreement with the findings in [5]. Of course, the proposed method for generating sampling patterns is not limited to parallel imaging methods; it can also be used for compressed sensing.

Conclusion

It is demonstrated in this paper that adapted variable density random sampling patterns can be generated with the use of template data sets. This approach yields results that are comparable to those of optimized model-based polynomial design strategies and shows pronounced improvements in comparison with non-optimized polynomial distributions. However, for the GRAPPA-based reconstruction used, no random sampling pattern showed superior performance when compared to conventional Cartesian subsampling and 2D CAIPIRINHA patterns.

Acknowledgments This work was supported by the Austrian Science Fund (FWF) under grant SFB F32 (SFB "Mathematical Optimization and Applications in Biomedical Sciences").

References

1. Pruessmann KP, Weiger M, Scheidegger MB, Boesiger P (1999) SENSE: sensitivity encoding for fast MRI. Magn Reson Med 42(5):952–962
2. Griswold MA, Jakob PM, Heidemann RM, Nittka M, Jellus V, Wang J, Kiefer B, Haase A (2002) Generalized autocalibrating partially parallel acquisitions (GRAPPA). Magn Reson Med 47(6):1202–1210
3. Glover GH, Noll DC (1993) Consistent projection reconstruction (CPR) techniques for MRI. Magn Reson Med 29(3):345–351
4. Lee JH, Hargreaves BA, Hu BS, Nishimura DG (2003) Fast 3d imaging using variable-density spiral trajectories with applications to limb perfusion. Magn Reson Med 50(6):1276–1285
5. Marseille GJ, de Beer R, Fuderer M, Mehlkopf AF, van Ormondt D (1996) Nonuniform phase-encode distributions for MRI scan time reduction. J Magn Reson B 111(1):70–75
6. Nayak KS, Nishimura DG (1998) Randomized trajectories for reduced aliasing artifact. In: Proceedings of the scientific meeting and exhibition of ISMRM, Sydney, Australia
7. Tsai CM, Nishimura DG (2000) Reduced aliasing artifacts using variable-density k-space sampling trajectories. Magn Reson Med 43(3):452–458
8. Greiser A, von Kienlin M (2003) Efficient k-space sampling by density-weighted phase-encoding. Magn Reson Med 50(6):1266–1275
9. Lustig M, Donoho D, Pauly JM (2007) Sparse MRI: the application of compressed sensing for rapid MR imaging. Magn Reson Med 58(6):1182–1195
10. Lustig M, Donoho DL, Santos JM, Pauly JM (2008) Compressed sensing MRI. IEEE Signal Process Mag 25(2):72–82
11. Breuer FA, Blaimer M, Mueller MF, Seiberlich N, Heidemann RM, Griswold MA, Jakob PM (2006) Controlled aliasing in volumetric parallel imaging 2D CAIPIRINHA. Magn Reson Med 55:549–556

12. Block KT, Uecker M, Frahm J (2007) Undersampled radial MRI with multiple coils. Iterative image reconstruction using a total variation constraint. Magn Reson Med 57:1086–1098

13. Lustig M, Pauly JM (2010) SPIRiT: iterative self-consistent parallel imaging reconstruction from arbitrary k-space. Magn Reson Med 64:457–471